Developing a Localized Prior Distribution for a Physics-Based Decline Curve Model – Application to Publicly Available Production Data from the Barnett Shale

ECEN 765 – Machine Learning with Networks – Final Project

Rafael Wanderley de Holanda
Texas A&M University
College Station, Texas
rafaelwh@tamu.edu

ABSTRACT

Decline curves are the simplest type of model to forecast production from oil and gas reservoirs. Based on a selected decline model and observed production data, a trend is projected to predict future well performance and reserves. Despite capturing general trends, these models are not sufficient to describe the underlying physics of complex multiphase porous media flow phenomena and to explain variations in production due to changes in operational conditions. The application of such models in a Bayesian framework is a feasible alternative to mitigate this issue and obtain more robust forecasts by considering a range of possible results. However, one important aspect that controls the predicted produced volumes and their uncertainty is the design of a suitable prior distribution, which can be quite subjective.

This paper presents a workflow for the development of a localized prior distribution for new wells drilled in shale formations which combines information gained from the previous production of surrounding wells and geospatial data (well surface and bottom coordinates). Such workflow aims to establish engineering criteria to reduce the subjectivity in the design of a prior distribution, reducing and reliably quantifying the uncertainty while assuming spatial continuity of specific decline curve parameters. A case study of 869 gas wells in the Barnett shale is presented.

KEYWORDS

probabilistic production forecast, localized prior, geostatistics

ACM Reference Format:
Rafael Wanderley de Holanda. 2017. Developing a Localized Prior Distribution for a Physics-Based Decline Curve Model – Application to Publicly Available Production Data from the Barnett Shale: ECEN 765 – Machine Learning with Networks – Final Project . In *Proceedings of Machine Learning with Networks (ECEN 765)*. ACM, New York, NY, USA, Article 4, 9 pages. https://doi.org/10.1145/nnnnnnn.nnnnnnn

ECEN 765, December 2017, College Station, Texas USA

ACM ISBN 978-x-xxxx-xxxx-x/YY/MM. . . $15.00
https://doi.org/10.1145/nnnnnnn.nnnnnnn

1 INTRODUCTION

It is important to forecast the oil and gas rates of producing wells in order to make financial forecasts and define strategies and contracts for produced volumes to be sold. However, the underlying physical mechanism generating the produced rates (i.e. porous media phenomena) is quite complex and comprised of several elements. Usually we cannot reliably quantify rock properties in the subsurface, so we rely on indirect estimates, we might have lab experiments for the fluid properties, we might decide to integrate all of this information into a single model. There are several types of reservoir models: decline curve models, material balance models, grid-based models, etc.. In this work, we focus on decline curve models; the premise is that we can extrapolate a trend of observed production rates based on a selected model, which is a simple equation. This practice has been applied since the beginning of the past century [1].

However, because these models are either empirical or based on a rough simplification of the physics controlling the porous media flow, it is useful to make such predictions considering a range of possible outcomes, instead of a deterministic predictions. In this sense, Gong et al. [4] has implemented Bayesian framework using the Markov chain Monte Carlo (MCMC) algorithm for uncertainty quantification. Further developments have been presented in [3] and [6]. However, in all of these implementations one of the most questionable points is how a prior distribution is defined and its impact on the overall uncertainty of the production forecasts.

In this work, a new methodology is introduced which generates a localized prior for each well to reduce uncertainty and capture local trends observed in the surrounding wells that were previously producing. This is important to enable more accurate estimates of produced volumes and clarify spatial patterns related to the production of wells in shale formations. The approach consists of a combination of the Bayesian approach (MCMC results) and mixture models with geostatistical techniques (variogram modeling and kriging), and requires only publicly available geospatial and production data.

2 METHODOLOGY

In this section, the workflow implemented for the design of a specialized prior distribution for each well is described.

Essentially, it consists of geostatistical results (simple kriging and variogram modeling) incorporated in a histogram-like distribution (more specifically, it can be called a "quantile distribution") while considering petroleum engineering concepts in the analysis (reservoir fluid type and fluid-flow model). In order to clarify the methodology with examples, the dataset and initial results are also presented in this section.

2.1 Physics-Based Decline Model

One of the advantages of a Bayesian framework is that it is a systematic way of quantifying uncertainty for model-based predictions. These models represent our understanding of the data generation mechanism. In the problem presented in this work, the data are publicly available gas monthly production (mscf/month) for 869 wells in the Barnett shale, where the well locations are shown in Fig. 1. The model used in this work was previously presented by Holanda et al. [6], and accounts for material balance and linear flow in these tight formations. Material balance is necessary to account for the fact that the reservoir is a finite resource; and linear flow is due to the fact that these are horizontal wells with multi-stage hydraulic fractures, which are necessary for economically feasible production in these tight formations. This physics-based model is the following infinite series:

$$q(t) = \frac{kA}{\mu L}\left(p_i - p_{wf}\right)\sum_{j=0}^{\infty} 2e^{-\frac{k}{\phi\mu c_t}\left(\frac{\pi}{2L}(1+2j)\right)^2 t}\cos\left(\frac{\pi}{2}\frac{x_i}{L}(1+2j)\right) \tag{1}$$

which can be written in a simpler way as the second Jacobi theta function (θ_2):

$$q(t) = q_i^*\theta_2\left(\chi, e^{-\eta t}\right) \tag{2}$$

This model has only three parameters for the curve fitting of the observed monthly production. q_i^* is the virtual initial rate:

$$q_i^* = \frac{kA}{\mu L}\left(p_i - p_{wf}\right), \tag{3}$$

χ is a parameter introduced to allow an initial delay and buildup in the production rates:

$$\chi = \frac{\pi}{2}\frac{x_i}{L}, \tag{4}$$

and η is the reciprocal characteristic time, which is related to the diffusivity constant of the reservoir:

$$\eta = \frac{\pi^2}{L^2}\frac{k}{\phi\mu c_t}. \tag{5}$$

For more detailed explanations and derivations of the θ_2 model, the reader is referred to [6]. Even though the θ_2 model is an infinite series, it can be computed in a timely manner via multi-precision algorithms. In this case study, a Mathematica built-in function is used for the implementation [10].

2.2 Organizing the Dataset: 869 Barnett Gas Wells

Our goal is to generate a specialized prior distribution for new wells drilled considering a general idea of typical values of the model parameters and the observed performance of surrounding wells up to the date of the beginning of the production. For this reason, first it is necessary to organize the data chronologically, subdividing hindcasts based on calendar dates, instead of number of producing months, as it had been done previously [6].

Additionally, the wells were divided into three groups according to the type of reservoir fluid (Fig. 2) because a previous analysis had pointed out that χ tends to have higher mean and larger variance as the liquid content increases [6](* journal version to be released soon). This classification is not based in any sophisticated algorithm, it is simply based on a pre-established range of initial producing gas liquid ratio [7], which is computed from the publicly available production data. The sequence of dry gas, wet gas and gas condensate windows as observed in Fig. 2 is in agreement with what is geologically expected.

2.3 Variogram Models

Since we have the well coordinates and a previous estimate of the decline curve parameters (η, χ and q_i^*), it is possible to analyze the spatial continuity of the parameters of the prior distribution (η, χ and $\frac{q_i^*}{q_{max}}$). Indeed, the maps shown in Fig. 3 for the P50 results previously obtained in [6] reveal that there is some spatial continuity. Therefore, we can take advantage of this fact to enhance our prior knowledge for new wells drilled.

Kriging is a technique for interpolating geospatial data in a new location given observations of surrounding locations. In this sense, before kriging is performed it is necessary to have a model that explains how the attributes are varying in space, this is known as a variogram model, which represents the spatial autcorrelation of the data [5]. However, before fitting a variogram model, it is recommended to transform the data into a standard distribution ($\mathcal{N}(0,1)$) performing a normal score transform, as shown in Fig. 4. So, the observed data is transformed by matching its quantiles to the ones of $\mathcal{N}(0,1)$. This is a non-parametric transformation, an interpolation function is generated to perform the normal score transform and another for its inverse.

Once the data has been normalized, we must fit a variogram model. There are different types of models that can be used, however the most common equations presented here have only two types of parameters: sill (C) and range (a). Sill corresponds to the total variance explained by a variogram model. Since variogram models can be summed, the summation of all of the sills must be equal to the variance of the sample. In our case, $\sum_j^v C_j = 1$ because the data has been normalized. The range adds a notion of the distance that the attributes are spatially correlated. In other words, large ranges mean good spatial continuity of the observed data and short ranges mean less continuity. Table 1 summarizes the types of variogram models used in this work, where γ is the variogram and h is the distance.

The software S-GeMS [9] was used to obtain variograms from the P50 estimates maps previously shown in Fig. 3,

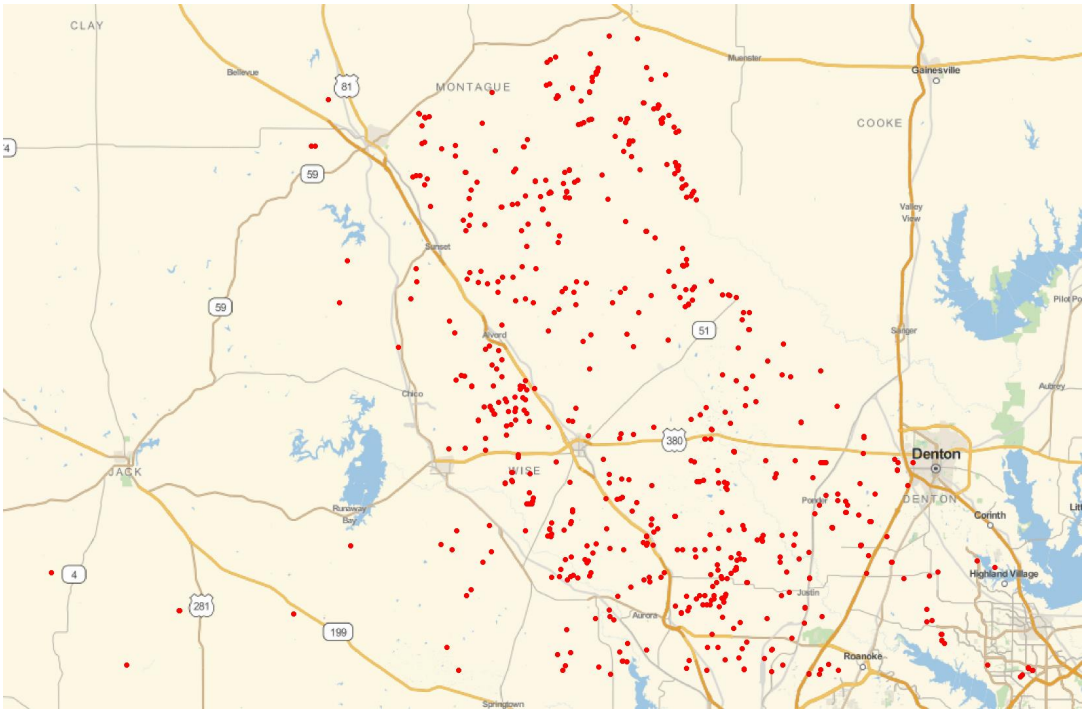

Figure 1: Locations for the 869 gas wells in the Barnett shale analyzed in this study.

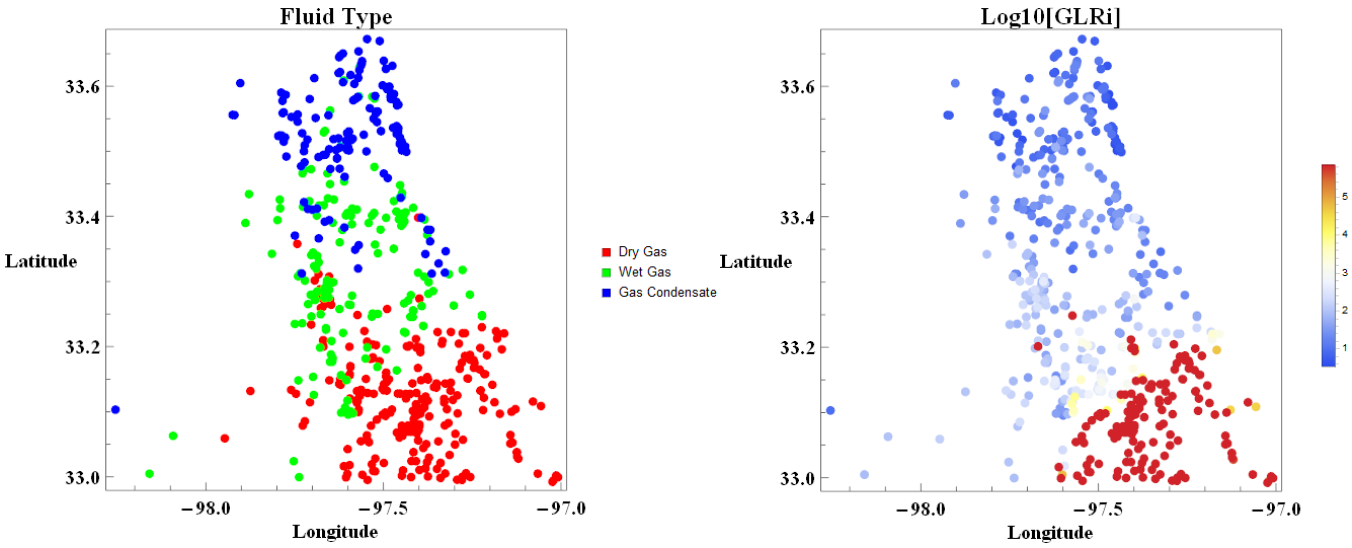

Figure 2: Reservoir fluid-type classification based on initial producing gas-liquid ratio (GLR_i).

which are presented in Tab. 2 for each reservoir fluid type. Figure 5 shows the model fitting to η_n^{-1} for dry gas wells.

2.4 Localized Simple Kriging

Once the variograms of the decline model parameters were obtained, kriging techniques allow to estimate their values at new well locations. There are several types of kriging methods [8], simple kriging was the one chosen for this work. The reason for this selection is discussed later on this text. Now, we focus on explaining the simple kriging equations.

For an attribute x_n, which is the normal score transform of x, the simple kriging estimate is given by:

$$x_{n,sk} = \bar{x}_n + \sum_{j=1}^{m} \lambda_j \left(x_{n,j} - \bar{x}_n \right) \tag{6}$$

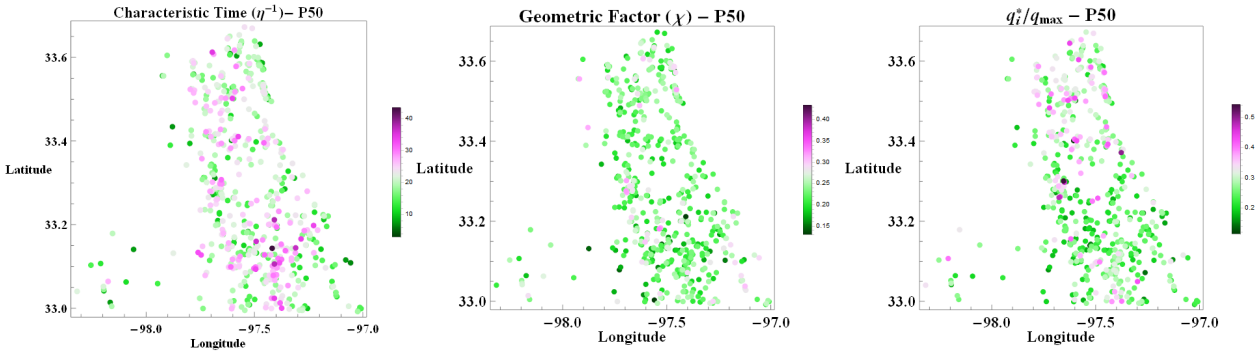

Figure 3: Maps with the P50 estimates of the decline curve parameters, some spatial patterns are observed reflecting on the performance of the wells.

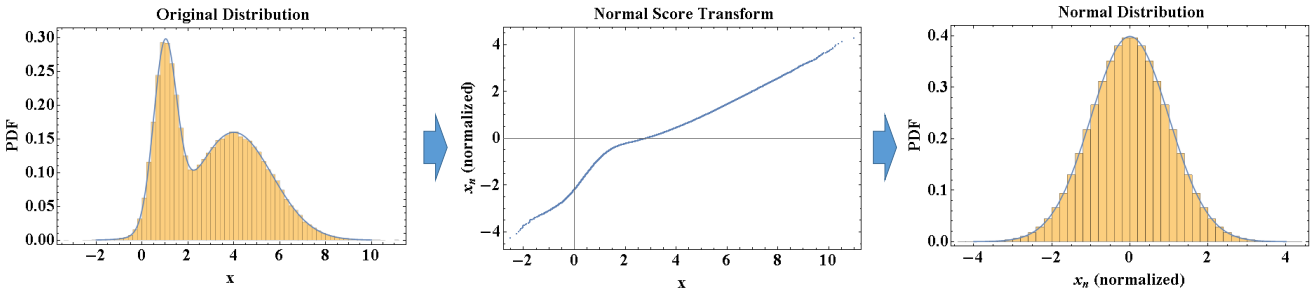

Figure 4: Example of normal score transform.

Table 1: Variogram models.

Variogram Type	Equation
nugget	$\gamma(h) = \begin{cases} 0, & h = 0 \\ C, & h > 0 \end{cases}$
exponential	$\gamma(h) = C\left(1 - e^{-3\frac{h}{a}}\right)$
Gaussian	$\gamma(h) = C\left(1 - e^{-3\left(\frac{h}{a}\right)^2}\right)$
spherical	$\gamma(h) = \begin{cases} C\left(\frac{3}{2}\frac{h}{a} - \frac{1}{2}\left(\frac{h}{a}\right)^3\right), & 0 \le h \le a \\ C, & h > a \end{cases}$

where $\bar{x}_n$ is a predefined average of x_n values, and λ are the kriging weights. Such weights are determined by minimizing the error variance of the estimates, which results in the following system of equations:

$$\begin{bmatrix} \sigma_{11} & \sigma_{21} & \cdots & \sigma_{m1} \\ \sigma_{12} & \sigma_{22} & \cdots & \sigma_{m2} \\ \vdots & \vdots & & \vdots \\ \sigma_{1m} & \sigma_{2m} & \cdots & \sigma_{mm} \end{bmatrix} \begin{bmatrix} \lambda_1 \\ \lambda_2 \\ \vdots \\ \lambda_m \end{bmatrix} = \begin{bmatrix} \sigma_{01} \\ \sigma_{02} \\ \vdots \\ \sigma_{0m} \end{bmatrix} \tag{7}$$

where σ_{ik} is the covariance between the i-th and k-th data points, and the new estimate is denoted as the 0-th data point. σ_{ik} can be calculated from the variogram model as follows:

$$\sigma_{ik} = \sum_{j=1}^{v} (C_j - \gamma_j(h_{ik})) \tag{8}$$

where v is the total number of variogram models summed to represent the spatial variability of the data. Since, the normal score transform has been applied, we have:

$$\sigma_{ik} = 1 - \sum_{j=1}^{v} \gamma_j(h_{ik}) \tag{9}$$

Therefore, a simple kriging estimate is obtained by substituting the results from Eqs. 9 and 7 in Eq. 6. Since we are mostly interested in identifying local trends of the parameters, we can reduce the number of data points used for kriging considering only the m closest ones, instead of all of them.

Table 2: Variogram models for prior parameters for each type of reservoir fluid.

Parameter	Nugget Effect	Variogram Type	Sill	Range (ft)
		Dry Gas		
η_n^{-1}	0.4	Exponential	0.6	33000
χ_n	0.6	Exponential	0.4	60000
$(q_i^*/q_{max})_n$	0.5	Exponential	0.5	60000
		Wet Gas		
η_n^{-1}	0	Exponential	1	2400
χ_n	0	Exponential	1	4800
$(q_i^*/q_{max})_n$	0	Exponential (1), Gaussian (2)	0.7 (1), 0.3 (2)	2400 (1), 40800 (2)
		Gas Condensate		
η_n^{-1}	0.15	Exponential	0.85	14100
χ_n	0.5	Gaussian	0.5	1080
$(q_i^*/q_{max})_n$	0	Spherical	1	5640

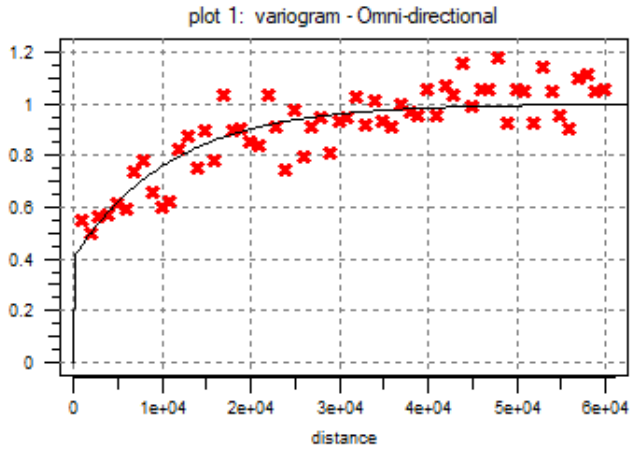

Figure 5: η_n^{-1} variogram model fitting for dry wells.

This reduces computational efforts for matrix inversion (Eq. 7) and emphasizes local trends. In this work, we set $m = 50$.

2.5 Prior Distribution

The Bayes theorem is used for uncertainty quantification of the production forecasts, which is essentially a combination of the prior knowledge ($P_{pr}(\mathbf{\Psi}_j)$), model selection and observed data (likelihood function, $P_l(\mathbf{q_{obs}}|\mathbf{\Psi}_j)$), generating a posterior distribution as follows [2]:

$$P_{post}(\mathbf{\Psi}_j|\mathbf{q_{obs}}) = \frac{P_l(\mathbf{q_{obs}}|\mathbf{\Psi}_j)P_{pr}(\mathbf{\Psi}_j)}{\int P_l(\mathbf{q_{obs}}|\mathbf{\Psi})P_{pr}(\mathbf{\Psi})d\mathbf{\Psi}} \tag{10}$$

where $\mathbf{\Psi}_j$ is a vector representing the parameters of a candidate model, e.g. $\mathbf{\Psi}_j = [\eta, \chi, q_i^*]_j^T$. While it is frequently impossible to obtain a closed-form solution to Eq. 10 because of the integral term in the denominator, the use of the Markov chain Monte Carlo algorithm (MCMC) enables to obtain large samples that follow $P_{post}(\mathbf{\Psi}_j|\mathbf{q_{obs}})$ [6].

In this subsection, we explain how the previously presented concepts (physics-based decline model, dataset, variograms, and kriging) are integrated in the design of a specialized prior distribution. First, we assume that the model parameters are independent:

$$P_{pr}(\mathbf{\Psi}_j) = P_{pr}(\eta_j)P_{pr}(\chi_j)P_{pr}(\mathbf{q_i}^*_j) \tag{11}$$

In our previous work [6], we assumed that each of the priors $P_{pr}(x)$ were determined by the best fit parametric PDF (amongst 26 types of distributions) to the histogram of the best fit decline models for all of the wells. So, we had a single prior that was applied to all of the wells. As previously mentioned, in this work, the data is subdivided in three classes of wells: dry gas, wet gas, and gas condensate. Then, a "general prior" was created for each of these classes based on the distribution of the best fit models. Instead of fitting

a parametric distribution to the histograms, we generate a mixture distribution [2]:

$$P_{pr}(x) = \sum_j P(x|j)P(j) \tag{12}$$

where j denotes the components of the mixture, $P(j)$ is the weight of each component, and $P(x|j)$ is the distribution that each component follows. In our case, for the "general prior", we are considering a mixture of uniform distributions that honors predefined quantiles of the dataset:

$$P_{pr}(x) = \sum_j P(j)\mathcal{U}(x_{j,min}, x_{j,max}) \tag{13}$$

We define a fixed interval between the quantiles (i.e. $P(j) = 0.1$ if we are considering all of the deciles). Then, we take the values of the attributes at these quantiles, i.e. $j \in$ [P10, P20, ..., P80, P90, P100], to set the minimum ($x_{j,min}$) and maximum ($x_{j,max}$) of the uniform distributions ($\mathcal{U}$) in such a way that always $x_{j-1,max} = x_{j,min}$. Additionally, $x_{P0,max}$ and $x_{P100,max}$ are the lower and upper constraints for the parameter x, respectively.

These general priors are assigned to the first wells starting production. For the succeeding wells, the specified quantiles (P10, ..., P90, P100) from the samples of the posterior distributions (obtained via MCMC) are used as kriging attributes, (x). Here, the simple kriging mean, $\bar{x}$ in Eq. 6, is defined as the equivalent quantile of the "general prior". Then, simple kriging is performed for all of the maps of the specified quantiles to estimate $x_{j,max}$ at the new well location. In this framework, the information is considered in a chronological way, the posterior of the surrounding producing wells is considering only production data up to the starting date of the new well for which we are designing a localized prior.

Thus, the prior for each parameter can be written as follows:

$$P_{pr}(x) = \sum_j P(j)\mathcal{U}(x_{j-1,sk}, x_{j,sk}) \tag{14}$$

We call it a "quantile distribution" because it honors the specified quantiles. Even though it has a histogram-like aspect, it is different from the common histogram distribution, which is usually based on a fixed bin width. For the MCMC implementation, one advantage of the quantile distribution as we defined is that the probability is never zero within solution space. On the other hand, the histogram distribution assigns zero probabilities to the bins lacking observations, which causes numerical instabilities in the MCMC algorithm. Figure 6 summarizes the workflow for the development of a localized prior.

3 RESULTS

Figure 7 shows the localized priors developed for all dry gas wells (on the right), which are derived from the "general prior" (on the left) and the kriging results from the posterior distributions of the surrounding wells. As observed, the localized priors fluctuate around the distribution of the "general prior". For several wells it becomes more confident (narrower) based on the evidence obtained from the trends of the production data of the surrounding wells. Therefore, the general prior sets a general trend from which adjustments are made based on the behavior presented by the wells in a specific region. If several wells previously drilled in that region present a similar production trend, gradually, we become more confident that the next well drilled there will behave likewise, which reflects in a narrower prior.

Figure 8 shows a measure of uncertainty which is the normalized P10-P90 range for the production during the second period (PDTSP) of the hindcasts. The uncertainty decreases significantly when the localized prior is applied compared to a single prior to all of the wells, as it had been done in our previous work [6].

It is also important to estimate if we are reliably estimating uncertainty, or if the methodology developed here tends to generate overconfident priors. Figure 9 shows a diagnostic plot to assess the validity of the uncertainty quantification. It is essentially checking the frequency that the produced volumes of probabilistic models are higher than the PDTSP for different periods used to fit the production history, considering all of the wells. For example, if the P50 models are calibrated, then, the will follow the 0.5 horizontal line in this plot, while the P10 and P90 should follow the 0.1 and 0.9 lines, respectively. Therefore, the deviations from these lines indicate if it is necessary to calibrate the uncertainty of the models. The case with a single prior had been previously calibrated in [6]. The case with the localized prior presents slighter deviations from the base case. However, this plot also indicates that we tend to become overconfident as the frequencies of the P10 models tend to higher values than 0.10 and the P90 models to lower values than 0.90. However, adjustments can be made to recalibrate uncertainty, as described in [6], by varying the heuristic weights assigned to production measurements. This process is computationally expensive, and is not justifiable here because we simply have a slight deviation. On the other hand, the uncertainty reduction (Fig. 8) was quite significant.

4 DISCUSSION

Simple kriging was used in this work because for data points that are distant from the observations (beyond the ranges of the variograms) it tends to the predefined mean values. Therefore, in these circumstances, the "general prior" is automatically assigned to the new wells. For this reason, we can say that the choice of simple kriging adds inertia to the "general prior". Additionally, a high nugget effect in the variograms also will tend to reconstruct a prior distribution very similar to the "general prior".

The variogram model has to be the same for all of the maps of the specified quantiles to ensure $x_{P90} < x_{P80} < ... < x_{P20} < x_{P10}$, so we always have $x_{j,min} < x_{j,max}$ in Eq. 13. In this work, we have used the variograms from the P50 estimates maps because the P50 results were better than the best fit results [6] and also the initial analysis of the maps the P50 estimates also presented clearer spatial patterns. The data used to generate these variograms models were the

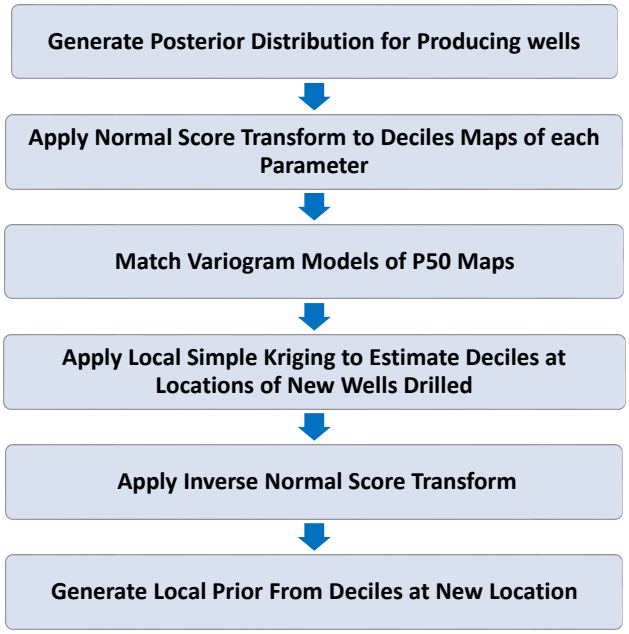

Figure 6: Workflow for the development of a localized prior.

estimates obtained from all of the production data available (no hindcast). However, this information will not be available since the beginning of the production, so the results will rely on an educated guess which might be based on some expected spatial trends from the geologic analysis. As more production data is gathered with time, it is recommended to readjust the variogram models.

Even though spatial continuity is the main assumption of this work, it is important to emphasize that we are looking at the problem from a probabilistic stand point, rather than deterministic. After a localized prior is designed, the model still has some freedom to fit the observed data (via the likelihood function). However, if our prior becomes too restrictive and presents low probability density for the maximum likelihood estimates (MLE), it will be necessary to acquire more data to have the maximum a posteriori (MAP) estimates converging to the observed values of production rates.

The spatial continuity assumption is based on the fact that some geological trends in petroleum reservoirs can be observed in a larger scale, which affects the production behaviors of the wells in a specific area. However, it is also important to mention that there are other factors that can impact the production; for example, the design of hydraulic fractures, number of stages, propped volume, and lateral length of the wells. Additionally, from a geological perspective, we can also observe local heterogeneities that impact fluid flow. Operational decisions and shut-in time can also affect the results.

The computational time has increased significantly for the analysis because the prior with the mixture of uniform distributions takes longer to compute than the parametric prior, which makes a difference in the MCMC algorithm. This is an aspect that can be improved in future implementations. A valuable question for future research is that if the use of this localized prior can help us to choose the most profitable places to drill a new with an inherent notion of the risk to be taken. Drilling a well costs millions of dollars, this might be a valuable tool to mitigate the risk when enough data is available.

5 CONCLUSIONS

- A workflow was developed to design a prior distribution for the parameters of a physics-based decline model taking into account the observed production of the surrounding wells up to the starting date of the new well.
- The assumption of spatial continuity is properly assessed through variogram models, which are matched to the parameter estimates available.
- The use of localized prior distributions reduces the uncertainty for the forecast of produced volumes.
- Analyzing information from geospatial and production data jointly improves our understanding of the Barnett shale, and allows the visualization of important spatial trends.

6 NOMENCLATURE

a : range, $[L]$

A : fracture face area, $[L^2]$

C : sill

c_t : total compressibility (rock and fluid), $[LT^2/M]$

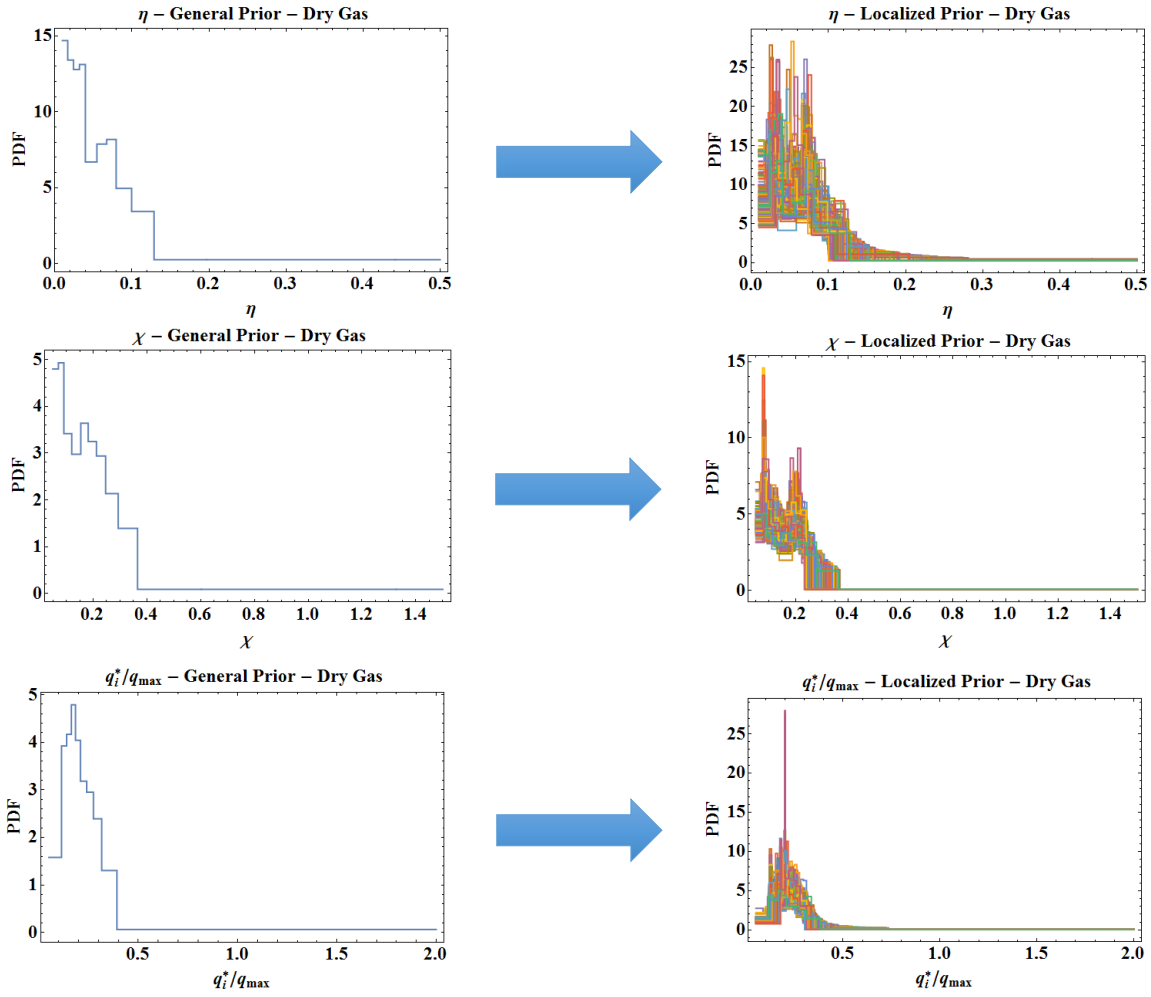

Figure 7: Prior distributions developed for dry gas wells: (left) "general prior"; (right) localized priors for all dry gas wells.

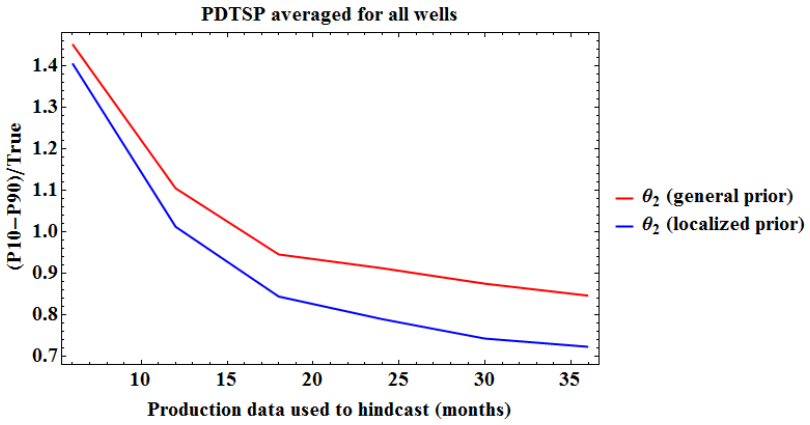

Figure 8: Uncertainty quantification for all of the wells comparing the use of a localized prior or a single prior to all of the wells.

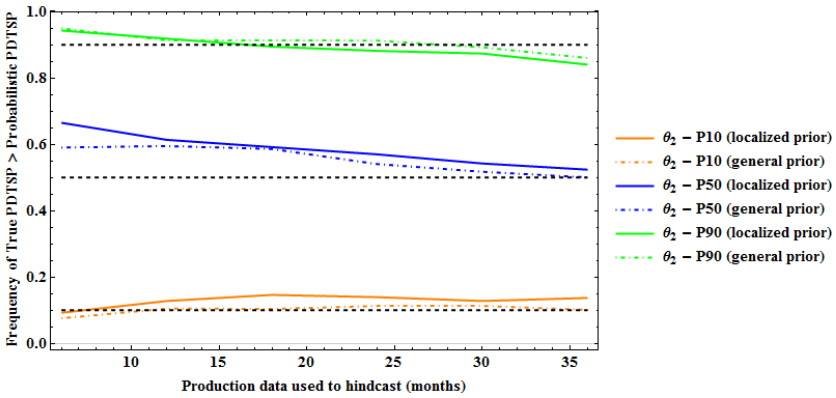

Figure 9: Uncertainty calibration of the hindcasts.

h : distance between attributes, $[L]$

k : matrix pemeability, $[L^2]$

L : reservoir length, $[L]$

$\mathcal{N}$: normal distribution

p_i : initial reservoir pressure, $[M/LT^2]$

p_{wf} : bottomhole flowing pressure, $[M/LT^2]$

q : well flowrate, $[L^3/T]$

q_i^* : virtual initial flowrate, $[L^3/T]$

q_{max} : maximum well flowrate, $[L^3/T]$

t : time, $[T]$

x : attribute

$\bar{x}$: attributes average for simple kriging

x_i : initial position, $[L]$

PDTSP : production during the second period

γ : variogram

η : reciprocal characteristic time, $[T^{-1}]$

θ_2 : Jacobi theta function no. 2

λ : kriging weights, $[dimensionless]$

μ : fluid viscosity, $[M/LT]$

σ : covariance

ϕ : matrix porosity, $[dimensionless]$

χ : geometric factor, $[dimensionless]$

subscripts and superscripts

m : number of points used for kriging

n : normal score transformed attribute

sk : simple kriging estimate

v : number of variogram models summed

REFERENCES

[1] J.J. Arps. 1945. Analysis of Decline Curves. *Petroleum Technology* 160, 01 (December 1945), 228–247. https://doi.org/10.2118/945228-G

[2] David Barber. 2012. *Bayesian reasoning and machine learning*. Cambridge University Press.

[3] David S. Fulford, Braden Bowie, Michael E. Berry, Bo Bowen, and Derrick W. Turk. 2016. Machine Learning as a Reliable Technology for Evaluating Time/Rate Performance of Unconventional Wells. *SPE Economics & Management* 8, 01 (January 2016), 23–39. https://doi.org/10.2118/174784-PA

[4] Xinglai Gong, Raul Gonzalez, Duane A. McVay, and Jeffery D. Hart. 2014. Bayesian Probabilistic Decline-Curve Analysis Reliably Quantifies Uncertainty in Shale-Well-Production Forecasts. *SPE Journal* 19, 06 (December 2014), 1047–1057. https://doi.org/10.2118/147588-PA

[5] E Gringarten, CV Deutsch, et al. 1999. Methodology for variogram interpretation and modeling for improved reservoir characterization. In *SPE annual technical conference and exhibition*. Society of Petroleum Engineers.

[6] Rafael Wanderley de Holanda, Eduardo Gildin, and Peter P. Valkó. 2017. Combining Physics, Statistics and Heuristics in the Decline Curve Analysis of Large Datasets in Unconventional Reservoirs. In *SPE Latin American and Caribbean Petroleum Engineering Conference* (2017). Society of Petroleum Engineers.

[7] William D McCain. 1990. *The properties of petroleum fluids*. PennWell Books.

[8] Michael J Pyrcz and Clayton V Deutsch. 2014. *Geostatistical reservoir modeling*. Oxford university press.

[9] Nicolas Remy. 2005. *S-GeMS: The Stanford Geostatistical Modeling Software: A Tool for New Algorithms Development*. Springer Netherlands, Dordrecht, 865–871. https://doi.org/10.1007/978-1-4020-3610-1_89

[10] Wolfram Research, Inc. 2015. *Mathematica*. version 10.3, Champaign, IL.